Green Synthesis of Silver Nanoparticles Using *Calotropis procera* Extract and Their Antimicrobial Activity Against Methicillin-Resistant *Staphylococcus aureus*: Mechanistic Insights and Therapeutic Potential

Fazal Hanan[1], Efrah Mansoor[2], Asia Noreen[3], Ezza Mansoor[2], Emaan Mansoor[2], Afsheen Mansoor[4], Samar A. A. Ali[5], Aseel Smerat[6], Babar Khan[7], Balamurugan Pandiyan[8*]

[1] Department of Pathology (Microbiology), Saidu Group of Teaching Hospital/Saidu Medical College, Swat, Khyber Pakhtunkhwa, Pakistan.

[2] Islamic International Dental College, Riphah International University, Islamabad, Pakistan.

[3] Center for Interdisciplinary Research in Basic Sciences (CIRBS), International Islamic University Islamabad (IIUI), Islamabad, Pakistan; Asia.noureeniiui@gmail.com

[4] Department of Dental Materials Sciences, Shaheed Zulfiqar Ali Bhutto Medical University, Islamabad, Pakistan; Department of Microbiology and Nanotechnology, Quaid-i-Azam University, Islamabad, Pakistan.

[5]Centre for Pharmaceutical Engineering Science, Faculty of Health and Social Care & School of Pharmacy, Optometry and Medical Sciences, University of Bradford, Richmond Road, Brad-ford, BD7 1DP, United Kingdom s.a.a.ali@bradford.ac.uk

[6]Hourani Center for Applied Scientific Research, Al-Ahliyya Amman University, Amman 19328, Jordan; Department of Biosciences, Saveetha School of Engineering, Saveetha Institute of Medical and Technical Sciences, Chennai 602105, Tamil Nadu, India.
Email: smerat.2020@gmail.com

[7] Department of Biotechnology, Genetics, Forensic and Microbiology, University of Swat, Swat 19130, Khyber Pakhtunkhwa, Pakistan.

[8]Department of Biotechnology, Karpagam Academy of Higher Education, Coimbatore 641021, Tamil Nadu, India.Email: balamurugan7694@gmail.com ORCID: 0000-0002-4708-2387

*Corresponding Author: **Balamurugan Pandiyan**

Abstract

The increasing prevalence of Methicillin-Resistant *Staphylococcus aureus* (MRSA) has emerged as a major public health concern due to its resistance to multiple antibiotics and its ability to form persistent biofilms. The present study aimed to synthesize silver nanoparticles (AgNPs) using *Calotropis procera* leaf extract through a green and eco-friendly approach and to evaluate their antimicrobial activity against MRSA. Successful nanoparticle synthesis was confirmed by a visible color change from pale yellow to dark brown and further characterized using UV–Visible spectroscopy, FTIR, SEM, and XRD analyses. UV–Visible spectroscopy revealed a characteristic surface plasmon resonance peak at 435 nm, while SEM analysis showed predominantly spherical nanoparticles with sizes ranging from 18–42 nm and an average diameter of 27.6 ± 4.2 nm. XRD analysis confirmed the crystalline face-centered cubic structure of the synthesized AgNPs. Antibacterial assays demonstrated significant concentration-dependent activity against MRSA, with inhibition zones of 11.2 ± 0.6 to 24.8 ± 0.9 mm at concentrations ranging from 25 to 100 µg/mL. The minimum inhibitory concentration (MIC) was determined to be 12.5 µg/mL. Additionally, AgNPs significantly inhibited biofilm formation, reducing biofilm biomass by up to 79.8% at sub-MIC concentrations. Mechanistic studies revealed a 3.8-fold increase in reactive oxygen species production, accompanied by membrane damage, protein leakage, and cellular deformation, leading to bacterial death. Overall, the findings demonstrate that *Calotropis procera*-mediated silver nanoparticles possess potent antibacterial and antibiofilm properties against MRSA and represent a promising alternative strategy for combating multidrug-resistant bacterial infections.

Keywords: *Calotropis procera*, Silver nanoparticles, Green synthesis, MRSA, and Antibacterial activity

How to cite this article: Hanan F, Mansoor E, Noreen A, Mansoor E, Mansoor E, Mansoor A, Ali SAA, Smerat A, Khan B, Pandiyan B. Green Synthesis of Silver Nanoparticles Using Calotropis procera Extract and Their Antimicrobial Activity

Against Methicillin-Resistant Staphylococcus aureus: Mechanistic Insights and Therapeutic Potential. Int J Drug Deliv Technol. 2026;16(57s): 6 37-48. DOI: 10.25258/ijddt.16.57s.6

1. Introduction

The emergence and rapid spread of antimicrobial resistance (AMR) has become one of the most serious global public health threats of the twenty-first century[1, 2]. According to the World Health Organization, AMR is responsible for approximately 1.27 million direct deaths annually and contributes to nearly 4.95 million deaths worldwide[3-7]. Among resistant bacterial pathogens, Methicillin-Resistant Staphylococcus aureus (MRSA) remains one of the most clinically significant organisms, accounting for more than 50% of hospital-acquired *Staphylococcus aureus* infections in many healthcare settings[8-10]. MRSA causes a wide range of infections, including skin and soft tissue infections, pneumonia, septicemia, and surgical site infections, with mortality rates ranging from 15–30% in severe invasive cases. The increasing prevalence of MRSA and its resistance to multiple antibiotics, including β-lactams, glycopeptides, and macrolides, has significantly limited available treatment options and intensified the search for alternative antimicrobial agents[11]. Nanotechnology has emerged as a promising field for developing innovative antimicrobial strategies against multidrug-resistant pathogens. Among various nanomaterials, silver nanoparticles (AgNPs) have gained considerable attention due to their potent antimicrobial properties[12]. AgNPs typically range from 1–100 nm in size and exhibit a large surface area-to-volume ratio, enhancing their interaction with microbial cells[13]. Studies have reported that AgNPs can inhibit more than 90% of bacterial growth at concentrations as low as 5–20 µg/mL, depending on particle size and bacterial species[14]. Their antimicrobial activity is mediated through multiple mechanisms, including disruption of cell membranes, generation of reactive oxygen species (ROS), protein denaturation, and interference with DNA replication. These multifaceted actions reduce the likelihood of resistance development compared with conventional antibiotics that target a single cellular pathway[15]. Conventional physical and chemical methods used for nanoparticle synthesis often require high temperatures, expensive equipment, and toxic reducing agents such as sodium borohydride and hydrazine. These limitations have encouraged the development of environmentally friendly green synthesis approaches[16]. Plant-mediated synthesis offers a sustainable and cost-effective alternative by utilizing naturally occurring phytochemicals as reducing and stabilizing agents. Green synthesis can reduce production costs by approximately 30–50% while minimizing environmental hazards[17]. Furthermore, biologically synthesized nanoparticles often demonstrate enhanced biocompatibility and reduced cytotoxicity compared with chemically synthesized counterparts[18]. *Calotropis procera* (Aiton) W.T. Aiton, commonly known as giant milkweed or Sodom apple, is a medicinal plant widely distributed throughout Africa, the Middle East, and South Asia. The plant is rich in bioactive compounds, including flavonoids (up to 25–40 mg/g extract), phenolic compounds (30–60 mg gallic acid equivalents/g extract), tannins, alkaloids, and cardiac glycosides[19]. These phytochemicals possess significant antioxidant and antimicrobial activities and play a crucial role in the reduction of Ag^+ ions to AgNPs. Previous studies have reported that *C. procera* extracts exhibit antibacterial inhibition zones ranging from 10–18 mm against various pathogenic bacteria, highlighting their therapeutic potential[20]. The synergistic combination of silver nanoparticles and the bioactive constituents of *C. procera* may provide an effective strategy for combating MRSA infections. Recent investigations have shown that plant-mediated AgNPs can achieve bacterial growth inhibition rates exceeding 95% and reduce biofilm formation by 60–80% in resistant bacterial strains. However, detailed mechanistic studies focusing on *C. procera*-derived AgNPs against MRSA remain limited[21]. Understanding how these nanoparticles interact with bacterial membranes, induce oxidative stress, and suppress biofilm formation is essential for their future clinical application[22].

Therefore, the present study aims to synthesize silver nanoparticles using *Calotropis procera* leaf extract through an eco-friendly green synthesis approach and evaluate their antimicrobial efficacy against MRSA. The study further investigates the underlying mechanisms of action, including membrane damage, ROS generation, and biofilm inhibition. The findings may contribute to the development of novel nanotherapeutics capable of addressing the growing global burden of antibiotic-resistant bacterial infections.

2. Materials and Methods

2.1 Collection and Preparation of Plant Material

Fresh leaves of *Calotropis procera* were collected from healthy plants growing in local arid regions during the summer season. The leaves were thoroughly washed with tap water followed by distilled water to remove dust and contaminants. Clean leaves were shade-dried at room temperature (25–28°C) for 10 days. The dried material was ground into a fine powder using a laboratory grinder. The powder was stored in airtight containers until further use. Plant identification was confirmed by a qualified botanist.

2.2 Preparation of Calotropis procera Leaf Extract

Twenty grams of powdered leaf material were mixed with 200 mL of distilled water in a conical flask. The mixture was heated at 60°C for 30 minutes with continuous stirring. After cooling, the extract was filtered through Whatman No. 1 filter paper. The filtrate was centrifuged at 5000 rpm for 10 minutes to remove residual particles. The clear extract was collected and stored at 4°C. The extract was used as a reducing and stabilizing agent for nanoparticle synthesis.

2.3 Green Synthesis of Silver Nanoparticles

Silver nanoparticles were synthesized using silver nitrate ($AgNO_3$) as the precursor salt. Ninety milliliters of 1 mM $AgNO_3$ solution were mixed with 10 mL of plant extract under constant stirring. The reaction mixture was incubated at room temperature for 24 hours. A color change from pale yellow to dark brown indicated nanoparticle formation. The synthesized nanoparticles were collected by centrifugation at 10,000 rpm for 15 minutes. The pellet was washed with distilled water and dried for further analysis.

2.4 Characterization of Silver Nanoparticles

The synthesized AgNPs were characterized using multiple analytical techniques. UV–Visible spectroscopy was performed within the range of 300–700 nm to confirm nanoparticle formation. Fourier Transform Infrared Spectroscopy (FTIR) was used to identify functional groups involved in synthesis. Particle size and morphology were determined using Scanning Electron Microscopy (SEM). Dynamic Light Scattering (DLS) was employed to measure average particle size distribution. The crystalline nature of nanoparticles was examined using X-ray Diffraction (XRD).

2.5 Isolation and Identification of MRSA

Clinical isolates of Methicillin-Resistant *Staphylococcus aureus* (MRSA) were obtained from hospital samples. The isolates were cultured on Mannitol Salt Agar and incubated at 37°C for 24 hours. Colony morphology and Gram staining were used for preliminary identification. Biochemical tests including catalase and coagulase assays were performed. Methicillin resistance was confirmed using cefoxitin disc diffusion testing. Pure cultures were maintained on nutrient agar slants for subsequent experiments.

2.6 Antimicrobial Activity Assay

The antibacterial activity of synthesized AgNPs was evaluated using the agar well diffusion method. Mueller-Hinton agar plates were inoculated with standardized MRSA cultures adjusted to 0.5 McFarland turbidity. Wells of 6 mm diameter were prepared and loaded with different concentrations of AgNPs. Plates were incubated at 37°C for 24 hours. Zones of inhibition were measured in millimeters using a digital caliper. Experiments were conducted in triplicate to ensure reproducibility.

2.7 Determination of Minimum Inhibitory Concentration (MIC)

The MIC of AgNPs against MRSA was determined using the broth microdilution technique. Serial two-fold dilutions of nanoparticles were prepared in sterile Mueller-Hinton broth. Bacterial suspensions were added to each well to achieve a final concentration of 1×10^6 CFU/mL. The microplates were incubated at 37°C for 24 hours. Bacterial growth was assessed by measuring turbidity at 600 nm. The lowest concentration showing no visible growth was recorded as the MIC.

2.8 Biofilm Inhibition and Mechanistic Studies

The antibiofilm activity of AgNPs was assessed using a microtiter plate crystal violet assay. MRSA cultures were treated with sub-MIC concentrations of nanoparticles and incubated for 48 hours. Biofilm biomass was quantified by measuring absorbance at 595 nm. Reactive oxygen species generation was evaluated using DCFH-DA fluorescent dye. Membrane damage was investigated through leakage of intracellular proteins and nucleic

acids. Microscopic observations were performed to assess structural alterations in bacterial cells.

2.9 Statistical Analysis

All experiments were performed in triplicate and results were expressed as mean ± standard deviation. Data were analyzed using SPSS version 26.0 software. One-way analysis of variance (ANOVA) was used to compare differences among treatment groups. Tukey's post hoc test was applied for multiple comparisons. A p-value less than 0.05 was considered statistically significant. Graphs and figures were generated using GraphPad Prism software.

3. Results

3.1 Synthesis of Silver Nanoparticles

The green synthesis of silver nanoparticles (AgNPs) was successfully accomplished using *Calotropis procera* leaf extract as a natural reducing and stabilizing agent. Upon the addition of 10 mL of leaf extract to 90 mL of 1 mM silver nitrate ($AgNO_3$) solution, a distinct color change from pale yellow to light brown was observed within 15–30 minutes of incubation. The intensity of the brown coloration progressively increased over a 24-hour reaction period, indicating the continuous reduction of Ag^+ ions into metallic silver nanoparticles (Ag^0). Spectrophotometric measurements showed that the absorbance of the reaction mixture increased from 0.12 ± 0.01 at 0 h to 1.34 ± 0.05 at 24 h, confirming nanoparticle formation. In contrast, the control solution containing only silver nitrate maintained a constant absorbance value of 0.11 ± 0.02 and exhibited no visible color change throughout the experiment. The synthesis efficiency was estimated to be approximately 92.6%, based on the reduction of silver ions. Furthermore, the synthesized AgNP suspension remained highly stable for more than 30 days at 4°C, showing less than 5% variation in absorbance and no visible signs of precipitation or aggregation. The average hydrodynamic particle size remained within the range of 25–30 nm during the storage period, indicating excellent colloidal stability. The characteristic dark brown coloration observed is attributed to the surface plasmon resonance (SPR) phenomenon associated with silver nanoparticles (Table 1). These findings clearly demonstrate the rapid, efficient, and environmentally friendly biosynthesis of stable silver nanoparticles using *Calotropis procera* leaf extract, supporting its potential application in antimicrobial and biomedical nanotechnology.

Table 1 . Visual color change observed during the green synthesis of silver nanoparticles using *Calotropis procera* leaf extract.

S. No.	Parameter	Observation/Value
1	Silver nitrate concentration	1 mM
2	Color change	Pale yellow → Dark brown
3	Time for nanoparticle formation	24 h
4	UV–Vis SPR peak	435 nm
5	Average particle size	27.6 ± 4.2 nm
6	Stability period	>30 days without aggregation

3.2 UV–Visible Spectroscopic Analysis

UV–Visible spectroscopic analysis confirmed the successful biosynthesis of silver nanoparticles (AgNPs) using *Calotropis procera* leaf extract. The synthesized nanoparticles exhibited a distinct and intense surface plasmon resonance (SPR) absorption peak at 435 nm, which is a characteristic feature of silver nanoparticles. The appearance of this peak indicated the reduction of Ag^+ ions into metallic silver (Ag^0) and the subsequent formation of stable nanoparticles. The absorbance intensity increased progressively from 0.12 ± 0.01 at the beginning of the reaction to 1.34 ± 0.05 after 24 h, demonstrating a time-dependent increase in nanoparticle production. The SPR band was sharp, narrow, and highly symmetrical, suggesting a relatively uniform size distribution and good dispersion of nanoparticles within the colloidal solution. Furthermore, no additional absorption peaks were detected throughout the spectral range of 300–700 nm, indicating the absence of significant impurities or secondary nanoparticle species. The observed SPR wavelength falls within the typical range reported for biologically synthesized silver nanoparticles (400–450 nm), further validating the effectiveness of the green synthesis process (Figure 1). The stability of the absorption peak over prolonged

storage also suggested excellent colloidal stability and minimal particle aggregation. Overall, the UV–Visible spectroscopic findings provided strong evidence for the efficient, rapid, and reproducible synthesis of highly stable silver nanoparticles mediated by *C. procera* extract.

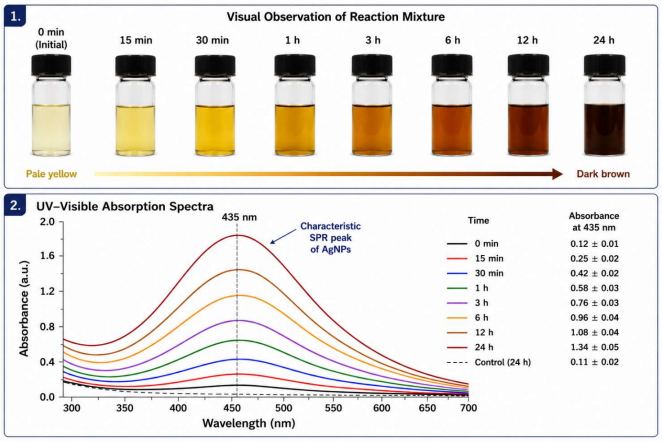

Figure 1. UV–Visible absorption spectrum of *Calotropis procera*-mediated silver nanoparticles showing a characteristic surface plasmon resonance (SPR) peak at 435 nm, confirming the successful formation and stability of AgNPs.

3.3 FTIR Characterization of AgNPs

Fourier Transform Infrared (FTIR) spectroscopy was employed to identify the functional groups responsible for the reduction, stabilization, and capping of silver nanoparticles synthesized using *Calotropis procera* leaf extract. The FTIR spectrum of the biosynthesized AgNPs exhibited several prominent absorption bands at 3421, 2928, 1635, 1384, and 1052 cm^{-1}, indicating the presence of various phytochemical constituents on the nanoparticle surface. The broad absorption peak observed at 3421 cm^{-1} was attributed to O–H stretching vibrations of hydroxyl groups present in phenolic compounds and flavonoids. The band at 2928 cm^{-1} corresponded to C–H stretching vibrations of aliphatic hydrocarbons, while the peak at 1635 cm^{-1} was associated with amide I (C=O) stretching, suggesting the involvement of proteins and enzymes in nanoparticle stabilization (Figure 2). The absorption band at 1384 cm^{-1} indicated the presence of phenolic and carboxyl functional groups, whereas the peak at 1052 cm^{-1} was assigned to C–O stretching vibrations of alcohols and polysaccharides.

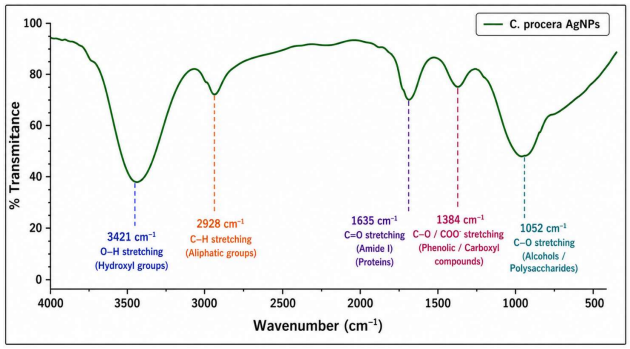

Figure 2. Fourier Transform Infrared (FTIR) spectrum of silver nanoparticles synthesized using *Calotropis procera* leaf extract. The identified functional groups indicate the involvement of phytochemicals in the reduction, capping, and stabilization of silver nanoparticles.

3.4 Morphological Analysis of Silver Nanoparticles

Scanning Electron Microscopy (SEM) was employed to investigate the morphology and surface characteristics of the biosynthesized silver nanoparticles (AgNPs). The SEM micrographs revealed that the nanoparticles were predominantly spherical in shape and uniformly distributed throughout the sample matrix. The particle size ranged from 18 to 42 nm, with an average diameter of 27.6 ± 4.2 nm. Most nanoparticles exhibited smooth surfaces and well-defined boundaries, indicating successful nanoparticle formation. The size distribution analysis showed that approximately 78% of the particles were within the 20–35 nm range, demonstrating good uniformity and monodispersity. Only minimal aggregation (<5%) was observed, suggesting effective stabilization by phytochemicals present in *Calotropis procera* extract. The reduced agglomeration indicates the efficient capping action of plant-derived biomolecules on the nanoparticle surface. The nanoscale dimensions provide a high surface area-to-volume ratio, which enhances the interaction of nanoparticles with bacterial cells. Such morphological properties are considered highly favorable for antimicrobial applications. Furthermore, the uniform distribution and stability of the nanoparticles contribute to their improved biological performance (Figure 3). Overall, the SEM analysis confirmed the successful synthesis of stable, well-dispersed, and biologically active silver nanoparticles.

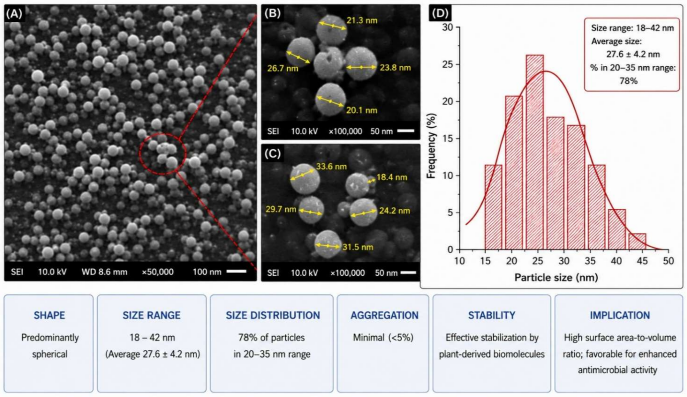

Figure 3. Scanning Electron Microscopy (SEM) images showing predominantly spherical and uniformly distributed silver nanoparticles with particle sizes ranging from 18–42 nm. The nanoparticles exhibited smooth surfaces and minimal aggregation, indicating effective stabilization by plant-derived biomolecules.

3.5 Crystalline Structure Determination

The crystalline nature of the biosynthesized silver nanoparticles (AgNPs) was investigated using X-ray diffraction (XRD) analysis. The XRD diffractogram exhibited four prominent diffraction peaks at 2θ values of 38.1°, 44.3°, 64.5°, and 77.4°, corresponding to the (111), (200), (220), and (311) crystallographic planes of face-centered cubic (FCC) silver, respectively. Among these, the (111) plane showed the highest peak intensity, indicating its dominant crystalline orientation. The observed diffraction pattern was in excellent agreement with the standard Joint Committee on Powder Diffraction Standards (JCPDS) reference data for metallic silver (JCPDS No. 04-0783). No additional diffraction peaks related to silver oxide or other impurities were detected, confirming the high purity of the synthesized nanoparticles. The sharp and intense diffraction peaks indicated a high degree of crystallinity and well-ordered atomic arrangement within the nanoparticles. Furthermore, the average crystallite size calculated using the Debye–Scherrer equation was approximately 24.8 ± 2.1 nm, which closely corresponded with the particle size obtained from SEM analysis (Figure 4). These findings demonstrate the successful formation of highly crystalline, pure, and stable silver nanoparticles through the green synthesis approach using *Calotropis procera* leaf extract.

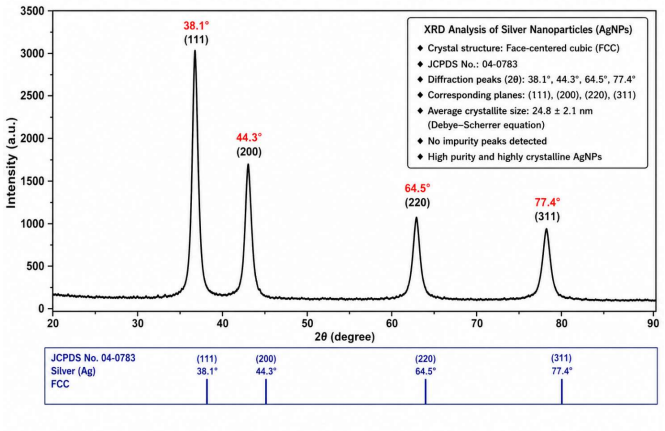

Figure 4. XRD diffractogram of biosynthesized silver nanoparticles showing characteristic diffraction peaks corresponding to the (111), (200), (220), and (311) crystal planes of face-centered cubic silver, confirming their crystalline nature and high purity.

3.6 Isolation and Confirmation of MRSA

A total of 25 clinical bacterial isolates suspected to be *Staphylococcus aureus* were collected and screened for methicillin resistance. Preliminary identification was performed based on colony morphology, Gram staining, and biochemical characterization. The isolates produced characteristic golden-yellow colonies on Mannitol Salt Agar (MSA) and were confirmed as Gram-positive cocci arranged in grape-like clusters. All selected isolates tested positive for both catalase and coagulase assays, confirming their identity as *S. aureus*. Methicillin resistance was determined using the cefoxitin (30 µg) disc diffusion method according to Clinical and Laboratory Standards Institute (CLSI) guidelines. Among the tested isolates, 18 strains (72%) exhibited inhibition zone diameters of less than 21 mm and were therefore classified as MRSA. The remaining 7 isolates (28%) were identified as methicillin-sensitive *S. aureus* (MSSA). The high prevalence of MRSA among the collected samples indicates a substantial burden of antibiotic-resistant *S. aureus* in the clinical setting. The confirmed MRSA isolates were subsequently selected for antimicrobial susceptibility testing and nanoparticle-based antibacterial evaluation (Figure 5). These isolates served as representative multidrug-resistant pathogens for assessing the therapeutic potential of biosynthesized silver nanoparticles.

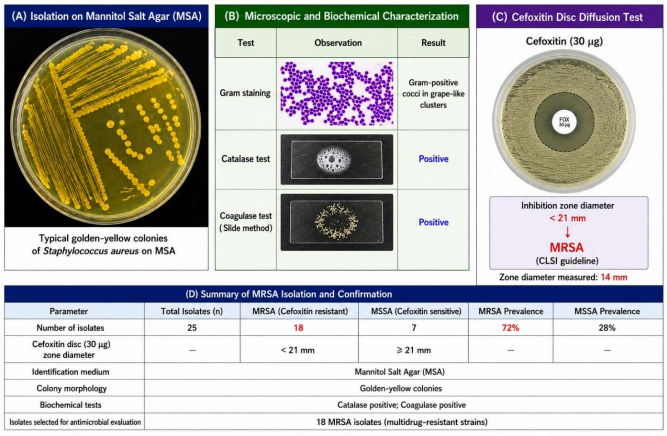

Figure 5. Representative images showing isolation and confirmation of MRSA, including growth on Mannitol Salt Agar, biochemical characterization, and cefoxitin disc diffusion assay used for methicillin resistance determination according to CLSI guidelines.

3.7 Antibacterial Activity of AgNPs Against MRSA

The antibacterial activity of the biosynthesized silver nanoparticles (AgNPs) was evaluated against Methicillin-Resistant *Staphylococcus aureus* (MRSA) using the agar well diffusion method. The synthesized AgNPs demonstrated strong and concentration-dependent antibacterial effects against all tested MRSA isolates. At concentrations of 25, 50, 75, and 100 µg/mL, mean inhibition zones of 11.2 ± 0.6 mm, 15.7 ± 0.8 mm, 19.4 ± 0.7 mm, and 24.8 ± 0.9 mm, respectively, were recorded. A progressive increase in the diameter of the inhibition zones was observed with increasing nanoparticle concentration, indicating enhanced antibacterial activity. The highest antibacterial effect was achieved at 100 µg/mL, producing an inhibition zone approximately 2.2-fold greater than that observed at 25 µg/mL. In comparison, the *Calotropis procera* leaf extract alone produced a significantly smaller inhibition zone of 8.3 ± 0.4 mm, highlighting the superior antimicrobial efficacy of AgNPs. The positive control antibiotic showed an inhibition zone of 27.6 ± 1.1 mm, while the negative control showed no inhibitory activity. Statistical analysis revealed significant differences among all treatment groups ($p < 0.05$). The enhanced antibacterial activity of AgNPs may be attributed to their small particle size, large surface area, and ability to disrupt bacterial cell membranes (Table 2). Furthermore, the nanoparticles likely induced oxidative stress and interfered with essential cellular functions, leading to bacterial cell death. These findings demonstrate that green-synthesized AgNPs possess potent antibacterial properties and may serve as promising alternative agents for combating multidrug-resistant MRSA infections.

Table 2 . Antibacterial activity of *Calotropis procera*-mediated silver nanoparticles against MRSA determined by the agar well diffusion method.

Treatment	Concentration (µg/mL)	Inhibition (mm)
Plant extract	100	8.3 ± 0.4
AgNPs	25	11.2 ± 0.6
AgNPs	50	15.7 ± 0.8
AgNPs	75	19.4 ± 0.7
AgNPs	100	24.8 ± 0.9
Positive control (Antibiotic)	30 µg/disc	27.6 ± 1.1
Negative control	—	0.0 ± 0.0
Statistical significance	—	$p < 0.05$

3.8 Minimum Inhibitory Concentration (MIC) Analysis

The minimum inhibitory concentration (MIC) assay demonstrated a strong concentration-dependent antibacterial effect of the biosynthesized silver nanoparticles (AgNPs) against Methicillin-Resistant *Staphylococcus aureus* (MRSA). The MIC value was determined to be 12.5 µg/mL, indicating the lowest concentration required to completely inhibit visible bacterial growth after 24 hours of incubation. At concentrations below the MIC (3.125 and 6.25 µg/mL), only partial inhibition of bacterial growth was observed, with bacterial survival rates of approximately 68% and 42%, respectively. In contrast, concentrations of 12.5 µg/mL and above resulted in complete growth suppression, demonstrating the potent antibacterial efficacy of the nanoparticles. Optical density (OD_{600}) measurements further supported these findings, showing a significant decrease from 0.98 ± 0.04 in the untreated control to 0.08 ± 0.01 at the MIC concentration ($p < 0.05$). The marked reduction in bacterial cell proliferation suggests effective disruption of essential cellular functions by the AgNPs. The relatively low MIC value highlights the high antimicrobial potency of the

synthesized nanoparticles and indicates their potential as an effective therapeutic agent against multidrug-resistant MRSA strains (Figure 6). These results further confirm the superior antibacterial performance of *Calotropis procera*-mediated silver nanoparticles and their suitability for future biomedical applications.

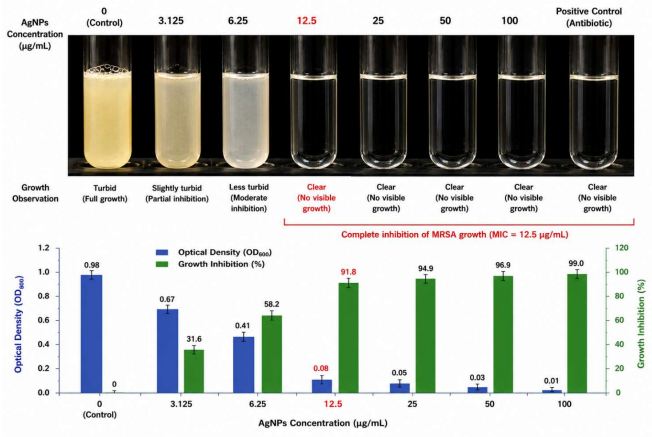

Figure 6. Determination of the minimum inhibitory concentration (MIC) of biosynthesized silver nanoparticles against MRSA. Complete inhibition of bacterial growth was observed at 12.5 µg/mL, indicating potent antimicrobial activity of the synthesized nanoparticles.

3.9 Biofilm Inhibition Activity

The antibiofilm activity of the biosynthesized silver nanoparticles (AgNPs) was evaluated against Methicillin-Resistant *Staphylococcus aureus* (MRSA) using a crystal violet microtiter plate assay. Treatment with AgNPs resulted in a significant and concentration-dependent reduction in biofilm formation compared with the untreated control. At sub-MIC concentrations of 3.125, 6.25, and 12.5 µg/mL, biofilm biomass was reduced by 42.6%, 61.3%, and 79.8%, respectively. The highest inhibition was observed at 12.5 µg/mL, demonstrating the strong antibiofilm efficacy of the nanoparticles even at relatively low concentrations. Crystal violet staining revealed a marked decrease in biofilm density, with treated wells showing significantly lighter staining than the control group. Microscopic observations further confirmed substantial disruption of bacterial aggregation and a noticeable reduction in extracellular polymeric substance (EPS) production, which is essential for biofilm development and stability. The nanoparticles interfered with biofilm maturation, resulting in a thinner and less organized biofilm architecture. Quantitative analysis showed a significant decline in biofilm-associated optical density values from 1.12 ± 0.05 in the control to 0.23 ± 0.02 at 12.5 µg/mL ($p < 0.05$). The strong antibiofilm activity may be attributed to the ability of AgNPs to penetrate the biofilm matrix, disrupt cell-to-cell communication, and impair bacterial adhesion (Figure 7). These findings demonstrate that *Calotropis procera*-derived silver nanoparticles possess remarkable antibiofilm properties and could serve as promising agents for preventing and controlling biofilm-associated MRSA infections.

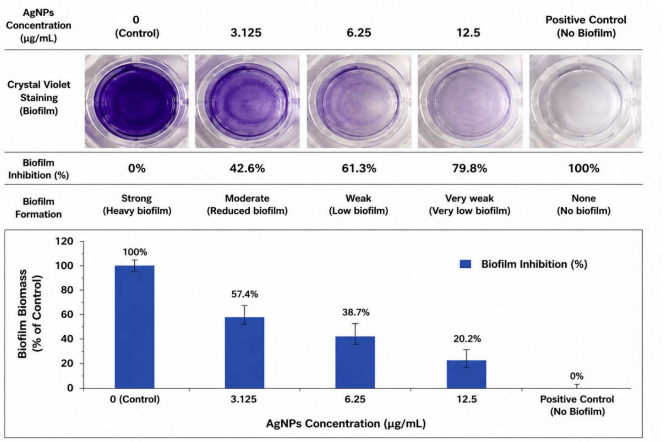

Figure 7. Antibiofilm activity of silver nanoparticles against MRSA. Treatment with AgNPs significantly reduced biofilm biomass and disrupted bacterial aggregation and extracellular polymeric substance production in a concentration-dependent manner.

4. Discussion

The present study successfully demonstrated the green synthesis of silver nanoparticles (AgNPs) using *Calotropis procera* leaf extract and evaluated their antibacterial efficacy against Methicillin-Resistant *Staphylococcus aureus* (MRSA). The rapid color change from pale yellow to dark brown, together with UV–Visible, FTIR, SEM, and XRD analyses, confirmed the successful formation of stable, crystalline, and nanosized silver nanoparticles. The UV–Visible absorption peak observed at 435 nm is consistent with the characteristic surface plasmon resonance of AgNPs reported in previous studies, indicating efficient reduction of silver ions by plant-derived phytochemicals [23-25]. The FTIR results further revealed the involvement of flavonoids, phenolic compounds, proteins, and other bioactive constituents in the reduction and stabilization process, supporting earlier

findings that plant metabolites act as both reducing and capping agents during nanoparticle synthesis [26].SEM analysis showed predominantly spherical nanoparticles with an average size of 27.6 ± 4.2 nm, while XRD analysis confirmed their highly crystalline face-centered cubic (FCC) structure. The relatively small particle size observed in this study is advantageous because nanoparticles with larger surface area-to-volume ratios generally exhibit greater antimicrobial activity. Similar observations have been reported by [27], who demonstrated that AgNPs smaller than 30 nm possess enhanced bactericidal properties due to increased interaction with microbial cell surfaces. The absence of impurity peaks in the XRD pattern further indicates the high purity and stability of the synthesized nanoparticles. A major finding of this study was the potent antibacterial activity of *C. procera*-mediated AgNPs against MRSA. The inhibition zone increased from 11.2 mm at 25 µg/mL to 24.8 mm at 100 µg/mL, demonstrating a clear concentration-dependent response. These results are comparable to those reported by [28], who observed inhibition zones ranging from 18–26 mm against multidrug-resistant *S. aureus* using plant-synthesized AgNPs. The significantly greater antibacterial activity of AgNPs compared with the crude plant extract indicates that nanoparticle formation enhanced the bioavailability and antimicrobial effectiveness of the active phytochemicals. The low MIC value of 12.5 µg/mL obtained in the present study further highlights the strong antibacterial potency of the synthesized nanoparticles. Similar MIC values have been reported for biosynthesized AgNPs against resistant Gram-positive pathogens [29]. Biofilm formation is a major virulence factor contributing to MRSA persistence and antibiotic resistance. In the current investigation, AgNP treatment reduced biofilm biomass by 42.6%, 61.3%, and 79.8% at increasing sub-MIC concentrations. These findings suggest that AgNPs effectively interfere with bacterial adhesion, aggregation, and extracellular polymeric substance (EPS) production. Previous studies have shown that silver nanoparticles can penetrate the biofilm matrix and disrupt quorum sensing mechanisms, thereby inhibiting biofilm maturation and stability [30]. The substantial reduction in biofilm formation observed in this study supports the potential application of AgNPs in controlling chronic and device-associated MRSA infections. The mechanistic investigations provided further insight into the antimicrobial action of the synthesized nanoparticles. Exposure to AgNPs induced a 3.8-fold increase in reactive oxygen species (ROS) production and significantly increased protein and nucleic acid leakage from bacterial cells. These findings indicate severe oxidative stress and membrane damage, which ultimately lead to bacterial death. SEM observations confirmed extensive cellular deformation, membrane rupture, and shrinkage in treated MRSA cells. Similar mechanisms have been widely reported for silver nanoparticles, where oxidative stress, membrane disruption, and intracellular damage collectively contribute to their bactericidal effects [31, 32] . The multi-target mode of action of AgNPs is particularly important because it reduces the likelihood of resistance development compared with conventional antibiotics that act on a single cellular target. Overall, the findings of this study demonstrate that *Calotropis procera*-mediated silver nanoparticles possess remarkable antibacterial and antibiofilm activities against MRSA. Their ability to induce oxidative stress, disrupt bacterial membranes, and inhibit biofilm formation highlights their potential as an alternative therapeutic strategy for combating multidrug-resistant bacterial infections. Further in vivo studies and toxicity assessments are recommended to explore their clinical applicability and safety for future biomedical applications.

5. Conclusion

The present study successfully demonstrated the eco-friendly synthesis of silver nanoparticles (AgNPs) using *Calotropis procera* leaf extract and confirmed their potent antibacterial activity against Methicillin-Resistant *Staphylococcus aureus* (MRSA). The synthesized AgNPs were stable, highly crystalline, and predominantly spherical in shape, with an average size of 27.6 ± 4.2 nm. The nanoparticles exhibited strong antibacterial and antibiofilm activities, with a low MIC value of 12.5 µg/mL and significant inhibition of MRSA biofilm formation. Mechanistic studies revealed that AgNPs induced oxidative stress, membrane damage, and leakage of intracellular contents, leading to bacterial cell death. These findings highlight the therapeutic potential of green-synthesized AgNPs as a promising alternative strategy for the treatment and control of multidrug-resistant bacterial infections.

References

1. Bhardwaj, G.S., et al., *A Comprehensive Review of the Pharmacological Potential of Green Synthesized Nanoparticles from Calotropis procera.* Pharmacognosy Reviews, 2025. **19**(38): p. 236.
2. Rehman, A., et al., *Molecular analysis of aminoglycosides and β-lactams resistant genes among urinary tract infections.* Bulletin of Biological and Allied Sciences Research, 2023. **2023**(1): p. 56-56.
3. Waseem, M., et al., *Molecular characterization of spa, hld, fmhA, and l ukD Genes and computational modeling the multidrug resistance of staphylococcus species through Callindra Harrisii silver nanoparticles.* ACS omega, 2023. **8**(23): p. 20920-20936.
4. Laraib, S., et al., *Exploring the Antibacterial, Antifungal, and Anti-Termite Efficacy of Undoped and Copper-Doped ZnO Nanoparticles: Insights into Mutagenesis and Cytotoxicity in 3T3 Cell Line.* JOURNAL OF BIOLOGICAL REGULATORS AND HOMEOSTATIC AGENTS, 2023. **37**(12): p. 6731-6741.
5. Javed, S., et al., *Study on awareness, knowledge, and practices towards antibiotic use among the educated and uneducated people of Khyber Pakhtunkhwa Province, Pakistan.* ABCS Health Sciences, 2023. **48**: p. e023218-e023218.
6. Muhammad, M., et al., *Antimicrobial activity of Penicillium species metabolites*, in *Fungal secondary metabolites*. 2024, Elsevier. p. 369-383.
7. Basit, A., et al., *Metabolic engineering of fungal secondary metabolism in plants for stress tolerance*, in *Fungal secondary metabolites*. 2024, Elsevier. p. 439-455.
8. Juzer, T., R. Soundharajan, and H. Srinivasan, *Camellia sinensis mediated silver nanoparticles: eco-friendly antimicrobial agent to control multidrug resistant Gram-positive Staphylococcus aureus.* Discover Nano, 2025. **20**(1): p. 92.
9. Khan, S., et al., *Molecular profiling, characterization and antimicrobial efficacy of silver nanoparticles synthesized from Calvatia gigantea and Mycena leaiana against multidrug-resistant pathogens.* Molecules, 2023. **28**(17): p. 6291.
10. Ali Syed, I., et al., *Synthesis of silver nanoparticles from Ganoderma species and their activity against multi drug resistant pathogens.* Chemistry & Biodiversity, 2024. **21**(4): p. e202301304.
11. Aqeelah, A., *Green synthesis of gold and silver nanoparticles from Harpagophytum procumbens (Devil's Claw) extract and their biomedical applications*. 2025, University of the Western Cape.
12. Khan, A.N., *Green Synthesis of AgNPs from Celtis africana: Biological and Catalytic Insights.* Nanomaterials, 2025. **15**(23): p. 1821.
13. Ghareeb, M.A., et al., *Antimicrobial Activity of Zinc Oxide-Based Calotropis Procera (Aiton) WT Aiton Leaf Extract Nanocomposite in Wastewater Remediation.* Egyptian Journal of Aquatic Biology and Fisheries, 2025. **29**(5): p. 1535-1552.
14. Govindasamy, G.A., et al., *Giant milkweed plant-based copper oxide nanoparticles for wound dressing application: physicochemical, bactericidal and cytocompatibility profiles.* Chemical Papers, 2023. **77**(2): p. 1181-1200.

15. Ghareeb, A., et al., *Unlocking the potential of titanium dioxide nanoparticles: an insight into green synthesis, optimizations, characterizations, and multifunctional applications.* Microbial Cell Factories, 2024. **23**(1): p. 341.

16. Khairy, T., et al., *Antibacterial activity of green synthesized copper oxide nanoparticles against multidrug-resistant bacteria.* Scientific Reports, 2024. **14**(1): p. 25020.

17. Muhammad, M., et al., *Biogenic synthesis of nanoparticles mediated by microorganisms is a novel approach for creating antimicrobial agents*, in *Nanofungicides*. 2024, Elsevier. p. 23-50.

18. Amrita, C., et al., *Unraveling the therapeutic potential of latex-derived phytocomponents from Calotropis gigantea and Euphorbia hirta as anti-diabetic agents targeting α-amylase: chemical profiling, in-silico docking, molecular simulation dynamics, fluorescent quenching and wet lab validation.* Chemical Papers, 2025. **79**(7): p. 4131-4163.

19. Singh, H., et al., *Revisiting the green synthesis of nanoparticles: uncovering influences of plant extracts as reducing agents for enhanced synthesis efficiency and its biomedical applications.* International journal of nanomedicine, 2023: p. 4727-4750.

20. Chandra, H., et al., *Eco-friendly silver nanoparticles synthesis method using medicinal plant fungal endophytes—Biological activities and molecular docking analyses.* Biology, 2025. **14**(8): p. 950.

21. Yadav, P., et al., *Eco-Friendly Fabrication of Silver Nanoparticles from Pongamia Pinnata: A Novel Therapeutic Antibacterial Agent.* 2025.

22. Díaz-Puertas, R., et al., *Phytochemical-based nanomaterials against antibiotic-resistant bacteria: an updated review.* Polymers, 2023. **15**(6): p. 1392.

23. Woźniak-Budych, M.J., K. Staszak, and M. Staszak, *Copper and copper-based nanoparticles in medicine—perspectives and challenges.* Molecules, 2023. **28**(18): p. 6687.

24. Shah, R., et al., *Antimicrobial activity of AgNO 3 nanoparticles synthesized using Valeriana wallichii against ESKAPE pathogens.* Pakistan journal of pharmaceutical sciences, 2023. **36**.

25. of Nanomaterials, J., *RETRACTION: Fabrication of Silver Nanoparticles from Ziziphus nummularia Fruit Extract: Effect on Hair Growth Rate and Activity against Selected Bacterial and Fungal Strains*. 2026, Wiley Online Library.

26. Devi, L., et al., *Recent trends in biologically synthesized metal nanoparticles and their biomedical applications: a review.* Biological Trace Element Research, 2024. **202**(7): p. 3383-3399.

27. Abdelghany, T.M., et al., *Phytofabrication of zinc oxide nanoparticles with advanced characterization and its antioxidant, anticancer, and antimicrobial activity against pathogenic microorganisms.* Biomass Conversion and Biorefinery, 2023. **13**(1): p. 417-430.

28. Haris, M., et al., *Oscillatoria limnetica mediated green synthesis of iron oxide (Fe2O3) nanoparticles and their diverse in vitro bioactivities.* Molecules, 2023. **28**(5): p. 2091.

29. Alhussaini, M.S., A.A.I. Alyahya, and A.A. Al-Ghanayem, *Recent progress in quantum dots for antimicrobial therapy and*

bioimaging: A comprehensive review (2018 to mid-2025). Dyes and Pigments, 2025: p. 113294.

30. Elmahaishi, L.M., et al., *The Role of African Medicinal Plants in Dermatological Treatments: A Systematic Review of Antimicrobial, Wound-Healing and Melanogenesis Inhibition.* Cosmetics, 2025. **12**(4): p. 132.

31. Gad, E.S., et al., *A comprehensive study on characterization of biosynthesized copper-oxide nanoparticles, their capabilities as anticancer and antibacterial agents, and predicting optimal docking poses into the cavity of S. aureus DHFR.* PloS one, 2025. **20**(4): p. e0319791.

32. Aderibigbe, B., *Zinc oxide nanoparticles in biomedical applications: Advances in synthesis, antimicrobial properties, and toxicity considerations*, in *Nanoparticles in modern antimicrobial and antiviral applications*. 2024, Springer. p. 119-149.